however, is smaller than a few percent in all cases, so it is not expected to be of any experimental significance. In the single-contact approximation, this concentration dependence disappears because the intramolecular segment distributions of the molecules in a pair are not perturbed in this approximation.

The numerical calculations are based on the two-chain Monte Carlo results of Olaj and co-workers[2-4] for $G(R)$, $\epsilon_{\parallel}(R)$, and $\epsilon_{\perp}(R)$ obtained by considering a chain with 50 steps on a cubic lattice, under both Θ and good solvent conditions. Therefore, the accuracy of the numerical estimates of the initial slopes of the single-chain properties as a function of concentration presented in this paper is restricted by the statistical accuracy of the computer results, especially at large separation distances. Furthermore, it is assumed that the shape of the functions $G(R)$, $\epsilon_{\parallel}(R)$, and $\epsilon_{\perp}(R)$ when they are expressed in terms of the normalized separation distance R/R_G is independent of molecular weight. It is desirable to check the validity of this assumption by repeating the two-chain Monte Carlo calculations with longer chains. As an independent test, we have calculated the interpenetration function

$$\psi = \frac{1}{2\pi^{1/2}} \int_0^\infty dX\, X^2(1 - G(X)) \qquad (41)$$

using the computer data for $G(X)$ and found $\psi = 0.29$, which is in fair agreement with experimental[19,23] as well as theoretical[24] values for the limit of the interpenetration function as the excluded volume parameter z goes to infinity. The discrepancy is perhaps due to the fact that the chain length is not sufficiently long (50-mers) and hence one is not quite in the large-z region. Extension of two-chain Monte Carlo calculations from Θ and good solvent conditions to intermediate solvents and parametrization of the pair distribution $G(R)$ at different temperatures are also desirable in the study of concentration dependence of static and dynamic chain properties in dilute solutions in general.

The concentration dependence of the static structure factor has also been studied by using two-chain Monte Carlo results without resorting to the single-contact approximation, and it was found that the shape of $S^{-1}(q;C)$ as a function of q^2 changes slightly with concentration, whereas it is independent in the conventional Zimm theory. The change seems to be large enough in the good solvent limit to be observed experimentally.

Acknowledgment. We express our gratitude to Professor Olaj and co-workers for making two-chain Monte Carlo results available to us. A.Z.A. thanks Dr. I. C. Sanchez from NBS for very fruitful discussions. B.H. is grateful to the Macromolecular Center (University of Michigan) for providing additional support. The help received at the beginning of this work from Dr. P. Goyal is also greatly appreciated. Acknowledgment is made to the donors of the Petroleum Research Fund, administered by the American Chemical Society, and to NBS for supporting A.Z.A. during the summer of 1982.

References and Notes

(1) Akcasu, A. Z. *Polymer* **1981**, *22*, 1169.
(2) Olaj, O. F.; Pelinka, K. H. *Makromol. Chem.* **1976**, *177*, 3413.
(3) Olaj, O. F.; Pelinka, K. H. *Makromol. Chem.* **1976**, *177*, 3447.
(4) Olaj, O. F.; Lantschbauer, N.; Pelinka, K. H. *Macromolecules* **1980**, *13*, 299.
(5) Zimm, B. *J. Chem. Phys.* **1946**, *14*, 164; **1948**, *16*, 1093.
(6) Okamoto, H. *J. Chem. Phys.* **1979**, *70*, 1690.
(7) Sanchez, I. C.; Lohse, D. J. *Macromolecules* **1981**, *14*, 131.
(8) Fixman, M. *Macromolecules* **1981**, *14*, 1710.
(9) Akcasu, A. Z. *Macromolecules* **1982**, *15*, 1321.
(10) Dubois-Violette, E.; de Gennes, P.-G. *Physics* **1967**, *3*, 181.
(11) Pyun, C. W.; Fixman, M. *J. Chem. Phys.* **1964**, *41*, 937.
(12) Kirkwood, J. G. *J. Polym. Sci.* **1954**, *12*, 1.
(13) Benmouna, M.; Akcasu, A. Z. *Macromolecules* **1978**, *11*, 1187.
(14) Akcasu, A. Z.; Han, C. C. *Macromolecules* **1979**, *12*, 276.
(15) Phillies, G. D. J. *J. Chem. Phys.* **1981**, *74*, 2346; **1981**, *75*, 508.
(16) Oono, Y. *J. Phys. Soc. Jpn.* **1978**, *41*, 228.
(17) de Gennes, P.-G. "Scaling Concepts in Polymer Physics"; Cornell University Press: Ithaca, NY, 1979.
(18) Lohse, D. J. *Macromolecules* **1981**, *14*, 1658.
(19) Yamakawa, H. "Modern Theory of Polymer Solutions"; Harper and Row: New York, 1971.
(20) Ohta, T.; Oono, Y.; Freed, K. F. *Phys. Rev. A* **1982**, *25*, 2801.
(21) Peterlin, A. *J. Chem. Phys.* **1955**, *23*, 2462.
(22) Akcasu, A. Z.; Benmouna, M. *Macromolecules* **1978**, *11*, 1193.
(23) Miyaki, Y.; Einaga, Y.; Fujita, H. *Macromolecules* **1978**, *11*, 1180.
(24) Freed, K. F. *J. Phys. A* **1982**, *15*, 1931.

Experimental Determination of the Temperature–Concentration Diagram of Daoud and Jannink in Two-Dimensional Space by Surface Pressure Measurements

Masami Kawaguchi,* Akira Yoshida, and Akira Takahashi

Department of Industrial Chemistry, Faculty of Engineering, Mie University, Tsu, Mie, 514 Japan. *Received September 9, 1982*

ABSTRACT: Surface pressure (π)–surface concentration (Γ) isotherms of poly(methyl acrylate) monolayers at the air–water interface were measured as functions of molecular weight and temperature in the vicinity of the Θ temperature. The crossover Γ^* between the dilute and semidilute regimes and the crossover Γ^{**} between the semidilute and concentrated regimes were determined. The π, Γ^*, Γ^{**}, and second virial coefficient A_2 data were compared with the theoretical predictions of Daoud and Jannink based on scaling concepts in two-dimensional space. The temperature dependences of these measured quantities were in good agreement with the theory, whereas the molecular weight dependence of these values did not agree with the theoretical calculations of Daoud and Jannink. A temperature–concentration diagram in two-dimensional space was drawn with the experimental results.

The scaling theories proposed by de Gennes[1] and the recently developed techniques of small-angle neutron scattering[2] and quasi-elastic light scattering[3] are making clear the thermodynamic, static, and dynamic properties of polymer solutions in the semidilute and concentrated (gel) regimes.

Daoud and Jannink[4] presented a temperature–concentration diagram of polymer solutions based on de Gennes'

0024-9297/83/2216-0956$01.50/0

suggestion that the Θ temperature is analogous to a tricritical point of a gas–liquid or magnetic system.[5] They defined four different regimes, consisting of dilute, semidilute, dilute tricritical, and semidilute tricritical (concentrated) regimes. For each of these regimes the mean square end-to-end distance, $\langle R^2 \rangle$, the screening length, ξ, and the osmotic pressure, π, were defined as functions of the degree of polymerization, N, polymer concentration, C, and reduced temperature, $\tau = T/\Theta - 1$, where T is the absolute temperature and Θ is the theta temperature. The second virial coefficient, A_2, was expressed as a function of N and τ. The exponents of N, C, and τ consist of the space dimensionality, d, the critical exponent of the excluded volume, ν, and the tricritical exponents of the excluded volume, ν_t, and crossover, ψ_t. Neutron scattering[6] and light scattering[7,8] studies have been carried out to test the predicted functional dependences of temperature and concentration of the important quantities $\langle R^2 \rangle$, ξ, and π describing polymer solution properties in three-dimensional space, i.e., $d = 3$.

However, in contrast with the three-dimensional space few experimental studies for Daoud and Jannink's relation in two-dimensional space have been reported. The surface polymer concentration dependence on the surface pressures of polymer monolayers under both good and Θ conditions was reported and the results were in good agreement with the predictions of the scaling laws for $d = 2$.[9,10]

According to the diagram of Daoud and Jannink, in two-dimensional space ($d = 2$), we have the temperature–concentration dependence of $\langle R^2 \rangle$, ξ, A_2, and π, which corresponds to the surface pressure of a polymer monolayer.

In a previous paper[10] we found that the Θ temperature of poly(methyl acrylate) monolayer at the air–water interface is 18.2 °C from plots of A_2 against the inverse of absolute temperature, and above 25 °C the good condition is well established. Therefore, the temperature range between 18.2 and 25 °C just corresponds to the poor condition between Θ and good conditions. The aim of this paper is to compare the temperature–concentration dependence of surface pressure and temperature dependence of A_2 of poly(methyl acrylate) monolayer at the air–water interface in the vicinity of the Θ point with the theoretical predictions of Daoud and Jannink. Furthermore, we will construct a temperature–concentration diagram in two-dimensional space.

Brief Outline of Daoud and Jannink's Theory

1. Dilute Regime. At low surface polymer concentration, Γ, the surface pressure, π, can be developed in powers of Γ using the virial expansion[11,12]

$$\pi/\Gamma RT = (1/M_n + A_{2,2}\Gamma + \ldots) \quad (1)$$

where R is the gas constant, T is the absolute temperature, M_n is the number-average molecular weight of the polymer, and $A_{2,2}$ is the second virial coefficient at the two-dimensional space. The value of M_n can be determined from the intercept of the plot of $\pi/\Gamma RT$ vs. Γ, and the slope of the plot gives the $A_{2,2}$ value.

Daoud and Jannink defined the second virial coefficient, $A_{2,d}$, in the general form as

$$A_{2,d} \sim N^{\nu d}\tau^{d(\nu-\nu_t)/\psi_t} \quad (2)$$

These exponents ν, ν_t, and ψ_t are calculated by the renormalization-group technique[1] with an expansion in $\epsilon = 3 - d$. For $d = 2$ the ϵ-expansion renormalization-group calculations predicted $\nu = 0.77$,[13] $\nu_t = 0.505$,[12] and $\psi_t = 0.60$.[14] Substitution of these numerical values of the exponents into eq 2 gives

$$A_{2,2} \sim N^{1.54}\tau^{0.88} \quad (3)$$

2. Semidilute Regime. The characteristic polymer concentration C^* where polymer chains begin to overlap corresponds to the crossover between the dilute and semidilute regimes. For concentrations above C^* the solution is defined to be in the semidilute regime. According to Daoud and Jannink the crossover polymer concentration C^* is defined as a function of molecular weight and temperature in the general form

$$C^* \sim N/R_{g,d}{}^d \sim N^{1-\nu d}\tau^{-d(\nu-\nu_t)/\psi_t} \quad (4)$$

with

$$R_{g,d} \sim N^{\nu}\tau^{(\nu-\nu_t)/\psi_t} \quad (5)$$

where $R_{g,d}$ is the radius of gyration of polymer in the dimensional space of d. For $d = 2$, we obtain the dependence of degree of polymerization and temperature on Γ* by substituting $\nu = 0.77$, $\nu_t = 0.505$, and $\psi_t = 0.60$ into eq 4

$$\Gamma^* \sim N^{-0.54}\tau^{-0.88} \quad (6)$$

For the semidilute regime Daoud and Jannink derived the temperature–concentration dependence of the osmotic pressure (surface pressure for $d = 2$) by using the relation that the free energy of the magnetic analogy is related to the osmotic pressure of the polymer solution, which was proposed by des Cloizeaux[15]

$$\pi/T \sim C^{\nu d(\nu d-1)}\tau^{(\nu-\nu_t)d/\psi_t(\nu d-1)} \quad (7)$$

Equation 7 can be rewritten by introducing $\nu = 0.77$, $\nu_t = 0.505$, and $\psi_t = 0.60$ for $d = 2$

$$\pi/T \sim \Gamma^{2.85}\tau^{1.64} \quad (8)$$

3. Concentrated Regime. Daoud and Jannink defined the crossover C^{**} between the semidilute and concentrated regimes as a function of reduced temperature, τ

$$C^{**} \sim \tau^{(\nu_t d-1)/\psi_t} \quad (9)$$

Above C^{**} the chains overlap but the Θ condition holds. Therefore, the concentrated regime corresponds to the semidilute regime at the Θ point, i.e., the semidilute tricritical regime, and the osmotic pressure π is defined as

$$\pi/T \sim C^{\nu_t d/(\nu_t d-1)} \quad (10)$$

For $d = 2$, we obtain the crossover line, Γ**, by substituting $\nu_t = 0.505$ and $\psi_t = 0.60$ into eq 9

$$\Gamma^{**} \sim \tau^{0.0167} \quad (11)$$

The surface pressure π is written by putting $\nu_t = 0.505$

$$\pi/T \sim \Gamma^{101} \quad (12)$$

Experimental Section

Materials. Poly(methyl acrylate) (PMA) was prepared by solution polymerization of freshly distilled methyl acrylate in benzene at 70 °C for 2 h using AIBN as an initiator. PMA was precipitated by methanol, dried under vacuum, dissolved in acetone, and separated into 10 fractions, using water as a precipitant at 25 °C. The number-average molecular weights of the fractionated samples were determined by a Knauer vapor pressure osmometer (VPO) in benzene at 37 °C and by a Hewlett-Packard 502 high-speed membrane osmometer (MO) in toluene at 30 °C. The polydispersity indices M_w/M_n of the samples were determined in THF at 38 °C by using a Toyo Soda HLC-802A gel permeation chromatography instrument. Five fractions were selected for the present investigation. The number-average molecular weights and the values of M_w/M_n of the samples are given in Table I.

Table I
Number-Average Molecular Weights and M_w/M_n of Poly(methyl acrylate)

sample	$M_n \times 10^{-3}$ VPO or MO	$M_n \times 10^{-3}$ surface pressure	M_w/M_n
PMA-1	2.7[a]	2.4	1.7
PMA-2	4.2[a]	3.8	1.1
PMA-3	5.3[a]	5.9	1.1
PMA-4	12.0[a]	9.5	1.1
PMA-5	30.2[b]		1.3

[a] VPO. [b] MO.

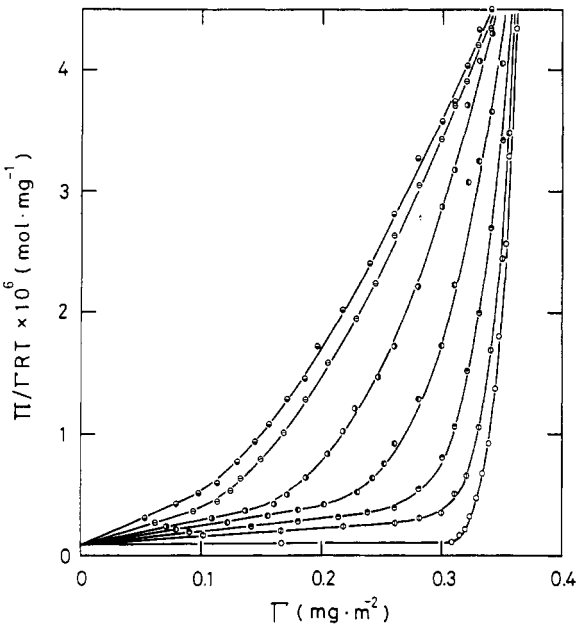

Figure 1. Plots of $\pi/\Gamma RT$ vs. Γ at different temperatures for PMA-4: (◒) 25 °C; (⊖) 22.5 °C; (◑) 21.0 °C; (◐) 20.2 °C; (◓) 19.5 °C; (⊕) 19.0 °C; (○) 18.2 °C.

Surface Balance. The surface pressures of the spread PMA monolayers were measured by the Wilhelmy technique using a glass plate attached to a sensitive torsion balance. The surface pressure was determined with a precision of $\pm 4 \times 10^{-5}$ N/m. A Teflon trough (0.16 m × 0.90 m × 0.01 m) was used. Double-distilled benzene was used as a spreading solvent and double-distilled water was used as the substrate. Spreading of the PMA on the water surface was carried out by applying 10-μL benzene solutions (0.5 mg/mL) of the polymers using a Terumo microsyringe. Compression of monolayers was carried out successively. The temperature of the substrate was controlled within 0.05 °C.

Results and Discussion

1. Dilute Regime. Examples of plots of $\pi/\Gamma RT$ vs. Γ at different temperatures for PMA-4 are shown in Figure 1. At low surface polymer concentration, the straight-line behavior clearly confirms eq 1 with intercept $1/M_n$ and slope $A_{2,2}$. From the intercept in Figure 1 we obtained $M_n = 9.5 \times 10^3$, which compares favorably with the value of M_n determined by vapor pressure osmometry. For other PMA samples similar plots were observed, but due to the uncertainty for low surface pressure, the value of M_n for PMA-5 could not be exactly determined. The values of M_n determined by the surface pressure measurements are listed in Table I. Their error was less than 10%.

As seen from Figure 1 the initial slope of the plot, which corresponds to $A_{2,2}$, increases with increasing temperature. Figure 2 shows plots of log $A_{2,2}$ vs. log ($\tau\Theta$) for PMA-1, -2, -3, -4, and -5. The error in $A_{2,2}$ for the low molecular weight samples PMA-1, -2, -3, and -4 is less than 10% but that for PMA-5 is less than 15%. Data points of $A_{2,2}$ for each polymer sample fall on the least-squares straight line with

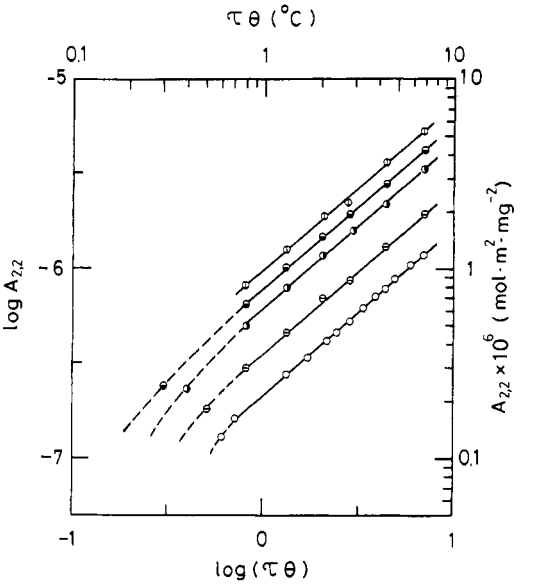

Figure 2. Double-logarithmic plots of the second virial coefficient $A_{2,2}$ vs. $\tau\Theta$: (○) PMA-1; (⊖) PMA-2; (◑) PMA-3; (◒) PMA-4; (⊕) PMA-5.

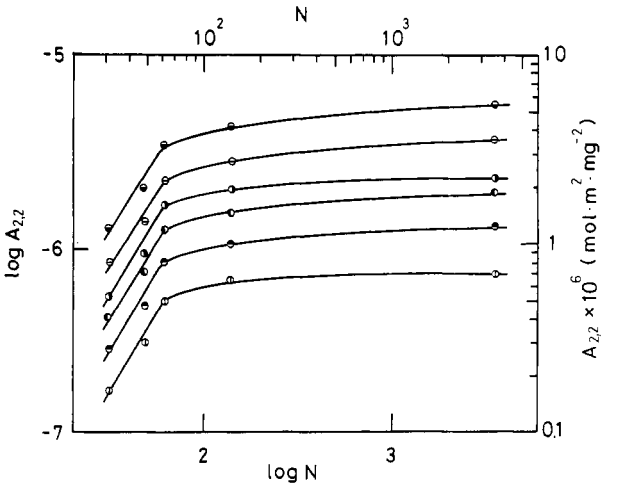

Figure 3. Double-logarithmic plots of $A_{2,2}$ vs. degree of polymerization N at different temperatures. Symbols are the same as in Figure 1.

slope 0.88 except for the $A_{2,2}$ obtained in the neighborhood of the Θ temperature ($0 < \tau\Theta < 1$ °C). The limit of error on the slope is found to be 0.88 ± 0.08. This value is in excellent agreement with the value of 0.88 predicted by eq 3.

The measured values of $A_{2,2}$ at constant temperature increase with increasing molecular weight. Equation 3 predicts that the value of $A_{2,2}$ increases in proportion with $N^{1.54}$. The measured $A_{2,2}$ at various temperatures are plotted against the degree of polymerization determined by VPO and MO in Figure 3. The data points increase linearly with molecular weight up to $M_n < 10^4$ and there is a definite leveling off in the high molecular weight region at respective temperatures. Therefore, in the dilute regime the temperature dependence of $A_{2,2}$ is in excellent agreement with the theoretical predictions of Daoud and Jannink, while the molecular weight dependence of $A_{2,2}$ is not in agreement with Daoud and Jannink's theory.

2. Semidilute Regime. By analogy to the definition of C^* in three-dimensional space, the value of the critical surface polymer concentration, Γ^*, in two-dimensional space may be estimated from the equation

$$\Gamma^* = M/(N_A \pi R_{g,2}^2) \quad (13)$$

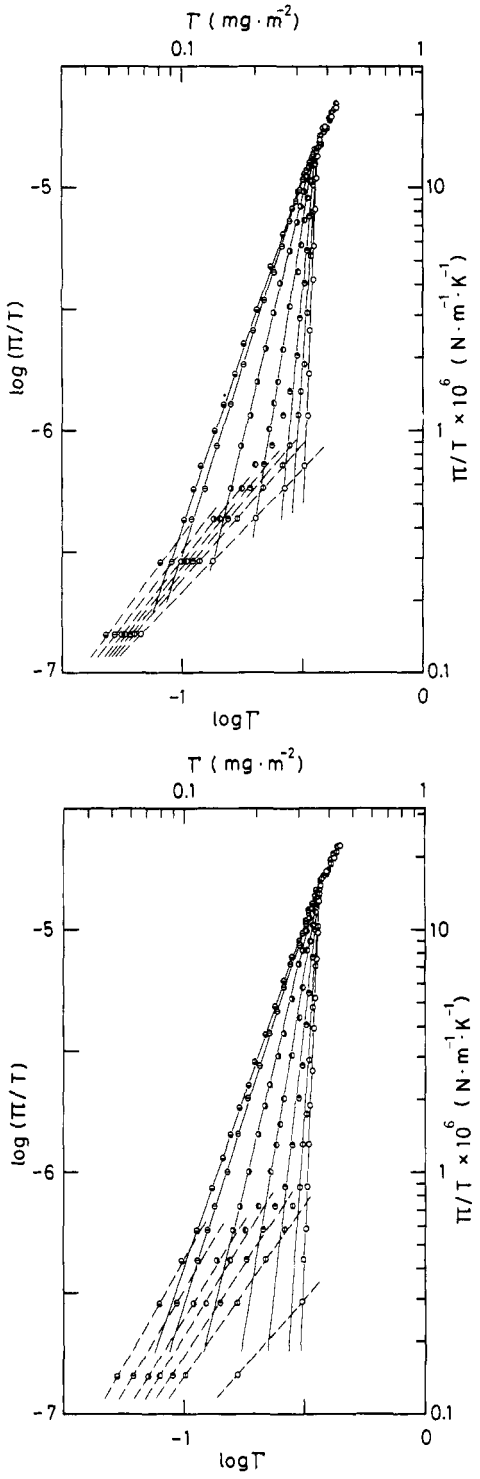

Figure 4. Double-logarithmic plots of π/T vs. Γ at different temperatures for PMA-2 (top) and PMA-4 (bottom). Symbols are the same as in Figure 1.

where N_A is Avogadro's number and $R_{g,2}$ is the radius of gyration in two-dimensional space. However, no adequate experimental method to measure $R_{g,2}$ is available at present, and we cannot estimate Γ^* from eq 13. In Figure 4, log (π/T) is plotted against log Γ for PMA-2 and PMA-4 at several temperatures. The data points describe a curve that first linearly increases with increasing Γ at lower polymer concentration, where eq 1 holds (dashed line), then deviates upward, and at still higher Γ changes to a new linear region (solid line) with a steeper slope than that of the initial part. The initial slope of the plot of log (π/T) vs. log Γ increases with increasing temperature, whereas

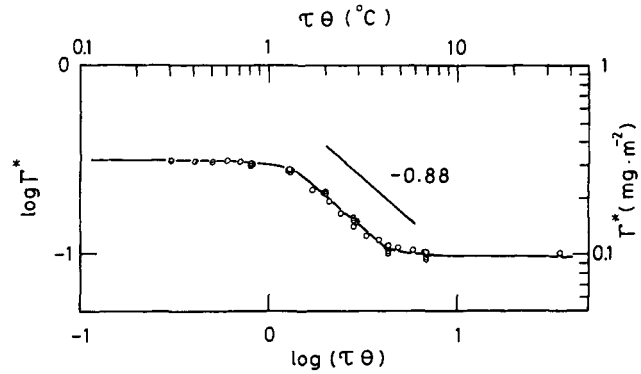

Figure 5. Double-logarithmic plots of Γ^* vs. $\tau\theta$. Symbols are the same as in Figure 2.

at higher surface polymer concentration the slope decreases with increasing temperature. We regard such a surface polymer concentration as Γ^* where the dashed line and solid line cross. The values of Γ^* determined by such a procedure are plotted against the temperature $\tau\theta$ on a double-logarithmic scale in Figure 5 for PMA-1, -2, -3, and -4. In the temperature range $1 < \tau\theta < 5$ °C, the data points fall on the least-squares straight line with slope −0.86 for the respective molecular weights. This value of the slope is in good agreement with eq 6. However, the Γ^* data for $\tau\theta < 1$ °C and $\tau\theta > 5$ °C deviate from the straight line and become independent of temperature. The Γ^* at the same temperature is almost independent of molecular weight.

As seen from Figure 4, above Γ^* the slope of the plot log (π/T) vs. log Γ decreases with increasing temperature and reaches a value of 2.85, which corresponds to the value of the slope under good conditions (eq 8).

In order to test the predicted value of 1.64 for the exponent of τ defined in eq 8, we show in Figure 6 examples of plots of log (π/T) vs. log $(\tau\theta)$ at several different surface polymer concentrations above Γ^* for PMA-1, -4, and -5. Below the surface polymer concentration of 0.320 mg/m^2 the data points for a finite temperature range fall on the least-squares straight line with slope 1.64 ± 0.02 irrespective of surface polymer concentration and molecular weight. The values of the slopes are in good agreement with eq 8. At lower temperature the values of log (π/T) deviate from the straight line, and at higher temperature log (π/T) becomes constant for the respective Γ. At constant Γ the temperature range that statisfies eq 8 becomes broader with increasing molecular weight. Above Γ = 0.330 mg/m^2, however, the slope of log (π/T) vs. log $(\tau\theta)$ plot decreases with increasing the surface polymer concentration, and at Γ = 0.360 mg/m^2, log (π/T) becomes almost constant and independent of log $(\tau\theta)$.

The surface concentration ranging from 0.330 to 0.360 mg/m^2 (Figure 4) may correspond to the crossover Γ^{**} between the semidilute and concentrated regimes. This result is in agreement with the fact that the crossover between the semidilute and concentrated regimes does not correspond to a sharp transition but to a rather smooth transition. Experimental determination of Γ^{**} will be discussed in a subsequent section to construct the temperature–concentration diagram in two-dimensional space.

3. Concentrated Regime. The data points depicted in Figure 4 converge in the neighborhood of a point with Γ = 0.36 mg/m^2 and $\pi = 4.2 \times 10^{-3}$ N/m irrespective of temperature and molecular weight, and beyond this point all the data almost fall on a master line. Since this convergence of data points satisfies eq 11, we regard the crossover Γ^{**} between the semidilute and concentrated regimes as the intercept of the solid lines drawn in Figure

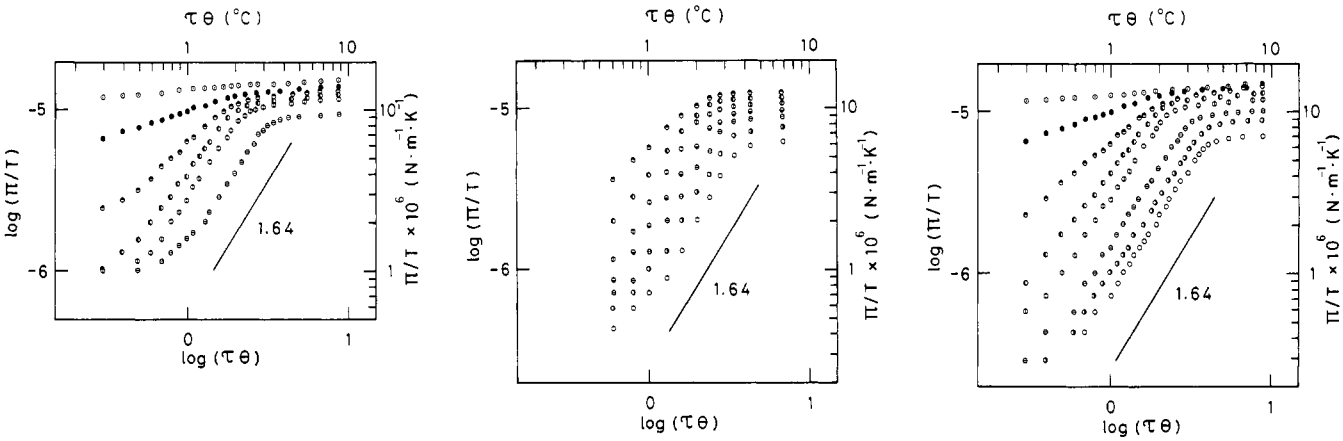

Figure 6. Double-logarithmic plots of π/T vs. $\tau\Theta$ at different surface polymer concentrations. (Left) PMA-1: (⊙) 0.36 mg/m^2; (●) 0.35 mg/m^2; (◒) 0.34 mg/m^2; (◐) 0.33 mg/m^2; (◑) 0.32 mg/m^2; (⊖) 0.30 mg/m^2. (Middle) PMA-4: (◒) 0.31 mg/m^2; (◑) 0.28 mg/m^2; (○) 0.26 mg/m^2. Other symbols are the same as for PMA-1. (Right) PMA-5: Symbols are the same as for PMA-1 and PMA-4.

Table II
Experimental Γ** Data as a Function of Temperature τΘ

	Γ**, mg/m^2				
τΘ, °C	PMA-1	PMA-2	PMA-3	PMA-4	PMA-5
0	0.35_6	0.36_3	0.36_3	0.35_5	0.36_5
0.7	0.36_0			0.35_5	
0.8		0.36_2	0.36_5		0.36_7
1.3	0.36_2	0.36_3	0.36_3	0.35_7	0.36_5
2.0		0.36_5	0.36_7		0.36_7
2.1				0.35_9	
2.8			0.37_1	0.36_3	0.37_1
2.9		0.36_2			
4.3		0.36_4	0.36_9		0.37_2
6.8	0.36_9	0.36_2	0.38_9	0.35_9	0.37_5

4 and the master line. The observed Γ** values are listed in Table II.

Above Γ** the slope of a straight line drawn in the plot of log (π/T) vs. log Γ is 2.10 ± 0.20. This value is much smaller than 101, which corresponds to the power for surface polymer concentration of the surface pressure in the concentrated regime obtained by Daoud and Jannink (see eq 12). This fact may indicate that the concentrated regime in two-dimensional space is not present for the monolayer of PMA spread at the air–water interface. For the structure of the PMA monolayer above Γ**, several explanations are plausible: first, formation of a partial multilayer structure; second, a partial submersion of the PMA chains; and last, formation of loop and train structure with large loop size. To determine the structure of PMA above Γ**, further studies are necessary.

4. Construction of Temperature–Concentration Diagram in Two-Dimensional Space. The temperature–concentration diagram in two-dimensional space is essentially determined by using the relations for the crossover lines Γ* and Γ** and the Γ_Θ* value predicted by Daoud and Jannink: The crossover line Γ* is given by eq 6. The crossover line Γ** is given by eq 11. Furthermore, the value of Γ_Θ* is given by

$$\Gamma_\Theta^* \sim N/R_{g,2\Theta}^2 \sim N/N^{2\nu_t} \qquad (14)$$

where $R_{g,2\Theta}$ is the radius of gyration in two-dimensional space under Θ conditions. Putting $\nu_t = 0.505$, one finds that Γ_Θ* is proportional to $N^{-0.01}$. Therefore, in order to construct a temperature–concentration diagram it is necessary to obtain the three quantities Γ*, Γ**, and Γ_Θ*. Experimental values of Γ_Θ* determined by the same procedure as for the determination of Γ* are listed in Table III and slightly decrease with increasing molecular weight.

Table III
Experimental Γ_Θ* Data

sample	Γ_Θ*, mg/m^2	sample	Γ_Θ*, mg/m^2
PMA-1	0.32_4	PMA-3	0.31_6
PMA-2	0.32_0	PMA-4	0.31_3

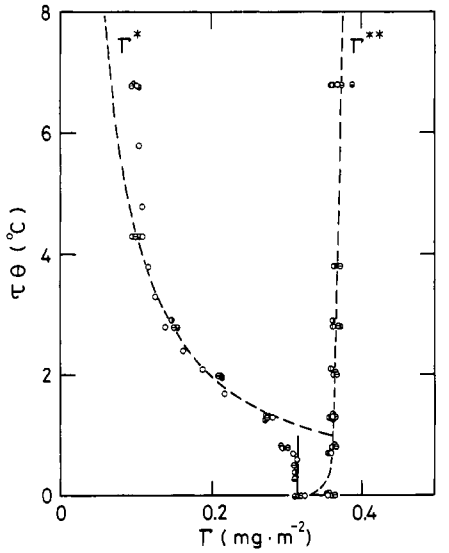

Figure 7. Temperature–concentration diagram of PMA monolayers at the air–water interface: Symbols are the same as in Figure 2. Dashed lines indicate the calculated Γ* and Γ** from the relations $\Gamma^* = 2.50 \times 10^{-3}\tau^{-0.88}$ and $\Gamma^{**} = 0.397\tau^{0.0167}$, respectively.

Since the important quantities Γ* and Γ** are available as a function of the reduced temperature, τ, we can easily construct a concentration–temperature diagram in two-dimensional space. Figure 7 shows a portion of the temperature–concentration diagram based on experimental data of Γ*, Γ**, and Γ_Θ* (on the abscissa). Since at constant temperature Γ* and Γ** are almost independent of molecular weight, the values of Γ* and Γ** fall on the respective master curves. As seen from Figure 7 the lines Γ* and Γ** do not intercept each other. This fact stems from the smaller measured exponent of 35 for the surface polymer concentration dependence of the surface pressure than the theoretical exponent of 101 at the Θ *condition*[10] (do not confuse with the exponent 101 above Γ** in eq 12). Below τΘ = 1.0 °C the constant Γ* values (vertical line) probably indicate that the dilute tricritical regime exists over a range of finite temperature ($0 < \tau\Theta < 1$ °C) as

suggested by Daoud and Jannink.[4]

Assuming that the simple relations $\Gamma^* = a^*\tau^{-0.88}$ and $\Gamma^{**} = a^{**}\tau^{0.0167}$ hold for the respective crossover lines, where a^* and a^{**} are numerical constants, we display the calculated values of Γ^* and Γ^{**} by the dashed lines in Figure 7. The values of a^* and a^{**} are selected to be 2.50×10^{-3} and 0.397, fitting the measured values in the experimental range of τ, respectively. Above $\tau\Theta = 5$ °C the measured values of Γ^* deviate from the calculated line Γ^* and have almost a constant value. This fact may reveal that the temperature range is not in the vicinity of the Θ temperature. In the range $0 < \tau\Theta < 1$ °C the measured value of Γ^* deviates downward from the calculated curve and falls on the vertical line separating a dilute tricritical regime and a concentrated regime.

Conclusions

By choosing relatively low molecular weight poly(methyl acrylate) samples, we determined definitely the crossover between the dilute and semidilute regimes and the crossover between the semidilute and concentrated regimes in two-dimensional space in the vicinity of the Θ temperature from surface pressure measurements. For each regime we have tested the theoretical predictions of Daoud and Jannink and obtained good agreement between experimental data and theoretical predictions for the temperature dependency. However, the molecular weight dependency is not in agreement with the theoretical predictions. Finally, we have constructed a temperature–concentration diagram of PMA monolayer using the experimental results. However, we could not confirm the existence of the concentrated regime.

Registry No. PMA, 9003-21-8.

References and Notes

(1) de Gennes, P.-G. "Scaling Concepts in Polymer Physics"; Cornell University Press: Ithaca, NY, 1979.
(2) Daoud, M.; Cotton, J. P.; Farnoux, B.; Jannink, G.; Sarma, G.; Benoit, H.; Duplessix, R.; Picot, C.; de Gennes, P.-G. *Macromolecules* **1975**, *8*, 804.
(3) Adam, M.; Delsanti, M. *Macromolecules* **1977**, *10*, 1229.
(4) Daoud, M.; Jannink, G. *J. Phys. (Paris)* **1976**, *37*, 973.
(5) de Gennes, P.-G. *J. Phys. (Paris), Lett.* **1975**, *36*, L-55.
(6) Cotton, J. P.; Nierlich, M.; Boué, F.; Daoud, M.; Farnoux, B.; Jannink, G.; Duplessix, R.; Picot, C. *J. Chem. Phys.* **1976**, *65*, 1101.
(7) Nose, T.; Chu, B. *Macromolecules* **1979**, *12*, 590. Chu, B.; Nose, T. *Ibid.* **1979**, *12*, 599.
(8) Munch, J. P.; Herz, J.; Boileau, S.; Candau, S. *Macromolecules* **1981**, *14*, 1370.
(9) Vilanove, R.; Rondelez, F. *Phys. Rev. Lett.* **1980**, *45*, 1502.
(10) Takahashi, A.; Yoshida, A.; Kawaguchi, M. *Macromolecules* **1982**, *15*, 1196.
(11) Huggins, M. L. *Makromol. Chem.* **1965**, *87*, 119.
(12) Stephen, M. J.; McCauley, J. *Phys. Lett. A* **1973**, *44*, 89.
(13) Le Guillou, J. C.; Zinn-Justin, J. *Phys. Rev. Lett.* **1977**, *39*, 95; *Phys. Rev. B* **1980**, *21*, 3976.
(14) Stephen, M. J. *Phys. Lett. A* **1975**, *53*, 363.
(15) des Cloizeaux, J. *J. Phys. (Paris)* **1975**, *36*, 281.

Estimating the Limiting Values of the Macroscopic Piezoelectric Constants of Poly(vinylidene fluoride) Form I

Kohji Tashiro and Hiroyuki Tadokoro*

Department of Macromolecular Science, Faculty of Science, Osaka University, Toyonaka, Osaka 560, Japan.

Received September 15, 1982

ABSTRACT: Limiting values of the macroscopic piezoelectric constants of poly(vinylidene fluoride) form I have been estimated: $d^{M}_{31} = 144.9$ pC/N, $d^{M}_{32} = 16.7$ pC/N, $d^{M}_{33} = -186.3$ pC/N, $e^{M}_{31} = 161.1$ mC/m^2, $e^{M}_{32} = 17.8$ mC/m^2, and $e^{M}_{33} = -202.5$ mC/m^2. The calculated values of $d^{M}_{31} = 145$ pC/N and electromechanical coupling constant $k^{M}_{31} = 63\%$ are comparable to those of piezoelectric inorganic materials such as Rochelle salt, PZT ($PbTiO_3/PbZrO_3$), and $BaTiO_3$ ceramics. An essential point in approaching the limiting values in the actual experiment is found to be how the degree of orientation of crystalline dipole along the electric field is increased during the poling process.

In a previous paper,[1] we discussed the origin of the piezoelectric effect in poly(vinylidene fluoride) (PVDF) form I from the molecular-theoretical point of view and estimated the role that the intrinsic piezoelectric effect of the crystalline region plays in the macroscopic piezoelectric effect. We proposed in that paper[1] that it is not an inherent piezoelectricity of the crystal but an electric and mechanical coupling between the polar crystal and nonpolar amorphous matrix that governs the essential features of the macroscopic piezoelectric phenomena. Such an idea of piezoelectric mechanism lead us to a good reproduction of the experimental values of the macroscopic piezoelectric constants as well as to an overall interpretation of the piezoelectric phenomena commonly observed for PVDF form I samples (e.g., the piezoelectric constant d^{M}_{31} is proportional to such factors as the content of polar form I crystal, the degree of dipole orientation along the electric field, the electrostriction constant, etc., and it also shows a large temperature dependence).[1]

The second important problem concerning the piezoelectricity of this polymer involves estimating the limiting values of the macroscopic piezoelectric constants. In the mechanical cases of ultrahigh-modulus polyethylene[2] and aromatic polyamides (Kevlar etc.),[3] the crystallite modulus or the Young's modulus of the crystalline region along the chain axis has supplied an important guiding measure as a limiting case for the production of polymer materials with much higher modulus. Similarly, an evaluation of limiting piezoelectric constants will give us a significant measure for the industrial production of effective piezoelectric polymer films. It may be also important in clarifying the situation of PVDF sample among a large number of piezoelectric materials. It should be noted here that, different from the case of Young's modulus, we need to estimate the limiting piezoelectric constants by taking into account the coupling effect of both the amorphous and crystalline phases and not simply the piezoelectric effect originating from the crystalline phase.

0024-9297/83/2216-0961$01.50/0